AN ACCURATE AND ADAPTIVE OPTICAL FLOW ESTIMATION ALGORITHM

Chin-Hung Teng, Shang-Hong Lai†, Yung-Sheng Chen‡, and Wen-Hsing Hsu**

*Department of Electrical Engineering, National Tsing Hua University, Hsinchu, Taiwan 300.
†Department of Computer Science, National Tsing Hua University, Hsinchu, Taiwan 300.
‡Department of Electrical Engineering, Yuan Ze University, Chung-Li, Taiwan 320.

ABSTRACT

In this paper we present a very accurate algorithm for computing optical flow with non-uniform brightness variations. The proposed algorithm is based on a generalized dynamic image model (GDIM) in conjunction with a regularization framework to cope with the problem of non-uniform brightness variations. To alleviate flow constraint errors due to image aliasing and noise, we employ a reweighted least-squares method to suppress unreliable flow constraints, thus leading to robust estimation of optical flow. In addition, a dynamic smoothness adjustment scheme is proposed to efficiently suppress the smoothness constraint in the vicinity of the motion and brightness variation discontinuities, thus preserving motion boundaries. To efficiently minimize the resulting energy function for optical flow computation, we apply an incomplete Cholesky preconditioned conjugate gradient algorithm to solve the large linear system. Experimental results on some synthetic and real image sequences show that the proposed algorithm outperforms most existing techniques reported in literature in terms of accuracy in optical flow computation with 100 % density.

1. INTRODUCTION

Without doubt, optical flow provides very important information for estimating 3D velocity fields, analyzing object motion, or segmenting images into regions based on their motions. A notable optical flow estimation algorithm is the gradient-based regularization method, which was proposed by Horn and Schunck [1]. In their method, the optical flow is estimated from the optical flow constraints, which is derived from the brightness constancy model (BCM), in conjunction with a first-order smoothness constraint.

Although the traditional gradient-based regularization method does not seem to perform well in benchmarking experimental comparison [2], Lai and Vemuri [3] demonstrated that, with an efficient algorithm, namely the incomplete Cholesky preconditioned conjugate gradient algorithm, the gradient-based regularization method can produce very accurate optical flow estimation. However, this gradient-based method suffers from the following problems. Firstly, due to BCM, the gradient-based approach is inaccurate when the image sequence contains brightness variations in the spatial or temporal domain. Secondly, this approach can not provide correct image motions in the vicinity of motion discontinuities owing to the smoothness assumption. Finally, the errors in the flow constraint due to numerical approximation, image aliasing and image noise also lead to inaccurate optical flow computation. Hence, to achieve very accurate optical flow estimation based on Lai and Vemuri's framework, these issues should be considered comprehensively.

In this work, we extend Lai and Vemuri's method to accommodate more realistic situations by taking all of the above issues into considerations. We employ the generalized dynamic image model to cope with the problem of non-uniform brightness variations. To alleviate flow constraint errors due to numerical approximation, image aliasing and noise, we employ a reweighted least-squares method to suppress unreliable flow constraints, thus leading to robust estimation of optical flow. Moreover, we also present a dynamic smoothness adjustment scheme to efficiently suppress the smoothness constraint at motion boundaries. In the following, the detailed formulation of these auxiliary estimation schemes and the minimization algorithm are described.

2. PROPOSED OPTICAL FLOW COMPUTATION

2.1. Energy Function Formulation

The original formulation of the gradient-based regularization method proposed by Horn and Schunck [1] involved minimizing an energy functional of the following form

$$\int_{\Omega} \left(I_x u + I_y v + I_t\right)^2 + \lambda\left(u_x^2 + u_y^2 + v_x^2 + v_y^2\right) d\mathbf{x}, \quad (1)$$

where I is the image intensity function, $\mathbf{u} = (u, v)$ is the motion vector field to be estimated, subscripts x, y and t denote the direction in the partial derivatives, λ is a parameter controlling the degree of smoothness. The optical flow constraint embedded in Eq. (1) is derived from BCM, which suffers from the problem of brightness variation. To account

0-7803-8554-3/04/$20.00 ©2004 IEEE.

for brightness variations, Negahdaripour proposed a generalized dynamic image model (GDIM) to estimate the generalized optical flow in dynamic imagery [4]. With GDIM, an extended optical flow constraint, $I_x u+I_y v+I_t+mI+c=0$ is developed, where m and c denote the multiplier and offset fields of the scene brightness variation field. Rather than minimizing the extended optical flow constraint directly, in this paper we minimize the minimum distance[1] between the flow vector and the linear flow constraint to amend the overweighting of the flow constraints at the high-gradient and high-intensity locations [3]. Thus, the energy function to be minimized can be written in a discrete form as follows,

$$\begin{aligned} f(\mathbf{u}) &= \sum_i \Big(\frac{I_{x,i}u_i + I_{y,i}v_i + I_{t,i} + m_i I_i + c_i}{\sqrt{I_{x,i}^2 + I_{y,i}^2 + I_i^2 + 1}}\Big)^2 \\ &+\lambda \sum_i \big(u_{x,i}^2 + u_{y,i}^2 + v_{x,i}^2 + v_{y,i}^2\big) \\ &+\mu \sum_i \big(m_{x,i}^2 + m_{y,i}^2 + c_{x,i}^2 + c_{y,i}^2\big), \end{aligned} \quad (2)$$

where i denotes the *i*-th location, vector $\mathbf{u}$ is the concatenation of all the flow components u_i, v_i, m_i and c_i, μ is a parameter controlling the degree of smoothness in m and c.

2.2. Robust Estimation

Robust estimation has been successfully applied in the computation of optical flow to alleviate large errors in the unreliable flow constraints [5]. In robust estimation, the square error function is replaced by a ρ-function to suppress the influence of the flow constraints with large residues on the estimated solution. Typical ρ-functions used in computer vision is the Lorentzian function, $\rho_{LO}(x) = \log(1 + \frac{x^2}{2})$. However, using the robust error function transfers the original energy function to non-convex, thus complicating the minimization algorithm in the optical flow estimation. Fortunately, a reweighted least-squares method [6] can be used to approximate the solution by minimizing the following weighted least-squares energy function iteratively,

$$\begin{aligned} f(\mathbf{u}) &= \sum_i w_i \Big(\frac{I_{x,i}u_i + I_{y,i}v_i + I_{t,i} + m_i I_i + c_i}{\sqrt{I_{x,i}^2 + I_{y,i}^2 + I_i^2 + 1}}\Big)^2 \\ &+\lambda \sum_i \big(u_{x,i}^2 + u_{y,i}^2 + v_{x,i}^2 + v_{y,i}^2\big) \\ &+\mu \sum_i \big(m_{x,i}^2 + m_{y,i}^2 + c_{x,i}^2 + c_{y,i}^2\big), \end{aligned} \quad (3)$$

where w_i is the weight for the *i*-th data constraint. For the Lorentzian function, the weight w_i is computed by $\frac{2\sigma^2}{2\sigma^2+{r_i}^2}$, where r_i is defined as $\frac{I_{x,i}\hat{u}_i+I_{y,i}\hat{v}_i+I_{t,i}+\hat{m}_i I_i+\hat{c}_i}{\sqrt{I_{x,i}^2+I_{y,i}^2+I_i^2+1}}$, and $\hat{u}_i$, $\hat{v}_i$, $\hat{m}_i$, and $\hat{c}_i$ are the previous estimated parameters. The scale parameter σ is selected as the standard deviation of r_i.

2.3. Dynamic Smoothness Adjustment

Lai and Vemuri's method can not give unambiguous image motions in the vicinity of motion discontinuity owing to the imposed smoothness constraint. In this paper, we develop a *dynamic smoothness adjustment* scheme to effectively suppress the smoothness constraint at the locations of motion boundaries and brightness variation discontinuities in the multiplier and offset fields. We control the strength of smoothness constraint by assigning an appropriate weight for each component of the constraint, thus obtaining the following energy function

$$\begin{aligned} f(\mathbf{u}) &= \sum_i w_i \Big(\frac{I_{x,i}u_i + I_{y,i}v_i + I_{t,i} + m_i I_i + c_i}{\sqrt{I_{x,i}^2 + I_{y,i}^2 + I_i^2 + 1}}\Big)^2 \\ &+\lambda \sum_i \big(\alpha_{x,i}u_{x,i}^2 + \alpha_{y,i}u_{y,i}^2 + \beta_{x,i}v_{x,i}^2 + \beta_{y,i}v_{y,i}^2\big) \\ &+\mu \sum_i \big(\gamma_{x,i}m_{x,i}^2 + \gamma_{y,i}m_{y,i}^2 + \delta_{x,i}c_{x,i}^2 + \delta_{y,i}c_{y,i}^2\big), \end{aligned} \quad (4)$$

where $\alpha_{x,i}$, $\alpha_{y,i}$, $\beta_{x,i}$, $\beta_{y,i}$, $\gamma_{x,i}$, $\gamma_{y,i}$, $\delta_{x,i}$ and $\delta_{y,i}$ are the weights for the corresponding components of the *i*-th smoothness constraint along *x*- and *y*- directions. In this research, we found that the angular deviation[2] between adjacent motion vectors is a good index for locating the motion discontinuities. Hence, we developed the following formulas to determine these weights.

$$\begin{aligned} r_i &= \theta_i - \bar{\theta}, \\ \theta_i &= \cos^{-1}\Big(\frac{\vec{v}_i \cdot \vec{v}_{i-1}}{|\vec{v}_i||\vec{v}_{i-1}|}\Big), \\ \alpha_{x,i} &= \begin{cases} \frac{2\sigma^2}{2\sigma^2+r_i^2}, & \text{if } r_i > 0, \\ 1, & otherwise, \end{cases} \end{aligned}$$

where $\vec{v}_i$ is defined as $(\hat{u}_i, \hat{v}_i, 1)$. The symbol θ_i is the angle between the vector $\vec{v}_i$ and its adjacent vector, $\vec{v}_{i-1}$, along *x* direction. Note that $\bar{\theta}$ is the mean of θ_i and σ is the standard deviation of θ_i. The weights $\alpha_{y,i}$ is determined similarly to that of $\alpha_{x,i}$ with $\vec{v}_{i-1}$ replaced by $\vec{v}_{i-h}$ (*h* is image height), the adjacent vector along *y*-direction. The other weights γ and δ also have the same form as those of α and β but with a different definition of θ_i. For determining $\gamma_{x,i}$, $\gamma_{y,i}$, $\delta_{x,i}$ and $\delta_{y,i}$, the values of θ_i are defined as $|\hat{m}_i - \hat{m}_{i-1}|$, $|\hat{m}_i - \hat{m}_{i-h}|$, $|\hat{c}_i - \hat{c}_{i-1}|$ and $|\hat{c}_i - \hat{c}_{i-h}|$,

[1] The minimum distance between (u_0, v_0, m_0, c_0) and $I_x u + I_y v + I_t + mI + c$ is $\frac{|I_x u_0+I_y v_0+I_t+m_0 I+c_0|}{\sqrt{I_x^2+I_y^2+I^2+1}}$.

[2] Here, we define the motion vector as $(u, v, 1)$, where (u, v) is the image motion. Thus, the image motions with the same orientation but different magnitude can also be distinguished by the angular deviations between them.

respectively. These formulas can assign small weights at the motion boundaries or brightness variation boundaries in the multiplier and offset fields. From our experiments, we found that this dynamic smoothness adjustment scheme can locate the motion boundaries correctly and greatly improve the accuracy of optical flow estimation.

3. NUMERICAL MINIMIZATION ALGORITHM

The energy function given by Eq. (4) can be rewritten as a matrix-vector form and minimizing this function is equivalent to solving a large linear system $\mathbf{Ku} = \mathbf{b}$. The vector $\mathbf{b} \in \Re^{4wh}$ (w and h are image width and height) is given by $\mathbf{b} = -[\mathbf{e}_{xt}^T \quad \mathbf{e}_{yt}^T \quad \mathbf{e}_{It}^T \quad \mathbf{e}_t^T]^T$, where $\mathbf{e}_{xt}$, $\mathbf{e}_{yt}$, $\mathbf{e}_{It}$ and $\mathbf{e}_t$ are all wh-dimensional vectors with entries $w_i I_{x,i} I_{t,i}/N_i$, $w_i I_{y,i} I_{t,i}/N_i$, $w_i I_i I_{t,i}/N_i$ and $w_i I_{t,i}/N_i$, respectively and $N_i = I_{x,i}^2 + I_{y,i}^2 + I_i^2 + 1$ is the normalization term. The matrix $\mathbf{K} \in \Re^{4wh \times 4wh}$ is symmetric positive-definite (SPD) and takes the following 4×4 block structure
$\mathbf{K} =$

$$\begin{bmatrix} \lambda\mathbf{K}_{s,\alpha} + \mathbf{E}_{xx} & \mathbf{E}_{xy} & \mathbf{E}_{xI} & \mathbf{E}_x \\ \mathbf{E}_{xy} & \lambda\mathbf{K}_{s,\beta} + \mathbf{E}_{yy} & \mathbf{E}_{yI} & \mathbf{E}_y \\ \mathbf{E}_{xI} & \mathbf{E}_{yI} & \mu\mathbf{K}_{s,\gamma} + \mathbf{E}_{II} & \mathbf{E}_I \\ \mathbf{E}_x & \mathbf{E}_y & \mathbf{E}_I & \mu\mathbf{K}_{s,\delta} + \mathbf{E} \end{bmatrix}, \tag{5}$$

where $\mathbf{E}_{xx}$, $\mathbf{E}_{xy}$, $\mathbf{E}_{xI}$, $\mathbf{E}_x$, $\mathbf{E}_{yy}$, $\mathbf{E}_{yI}$, $\mathbf{E}_y$, $\mathbf{E}_{II}$, $\mathbf{E}_I$ and $\mathbf{E}$ are all $wh \times wh$ diagonal matrices with diagonal entries $w_i I_{x,i}^2/N_i$, $w_i I_{x,i} I_{y,i}/N_i$, $w_i I_{x,i} I_i/N_i$, $w_i I_{x,i}/N_i$, $w_i I_{y,i}^2/N_i$, $w_i I_{y,i} I_i/N_i$, $w_i I_{y,i}/N_i$, $w_i I_i^2/N_i$, $w_i I_i/N_i$ and w_i/N_i, respectively. The matrices $\mathbf{K}_{s,\alpha}$, $\mathbf{K}_{s,\beta}$, $\mathbf{K}_{s,\gamma}$, and $\mathbf{K}_{s,\delta}$ come from the smoothness constraint and are determined by carefully expanding Eq. (4) and arranging α, β, γ and δ at corresponding locations of $\mathbf{K}$.

In this paper, we apply the preconditioned conjugate gradient algorithm with an incomplete Cholesky preconditioner $\mathbf{P}$ [3] to solve this linear system efficiently. The detailed steps of this algorithm (ICPCG) are described as follows:

1. Initialize $\mathbf{u}_0$; compute $\mathbf{r}_0 = \mathbf{b} - \boldsymbol{K}\mathbf{u}_0$; $k = 0$.
2. Solve $\boldsymbol{P}\mathbf{z}_k = \mathbf{r}_k$; $k = k + 1$.
3. If $k = 1$, $\mathbf{p}_1 = \mathbf{z}_0$; else compute $\beta_k = \mathbf{r}_{k-1}^T \mathbf{z}_{k-1} / \mathbf{r}_{k-2}^T \mathbf{z}_{k-2}$, and update $\mathbf{p}_k = \mathbf{z}_{k-1} + \beta_k \mathbf{p}_{k-1}$.
4. Compute $\alpha_k = \mathbf{r}_{k-1}^T \mathbf{z}_{k-1} / \mathbf{p}_k^T \boldsymbol{K} \mathbf{p}_k$.
5. Update $\mathbf{r}_k = \mathbf{r}_{k-1} - \alpha_k \boldsymbol{K}\mathbf{p}_k$, $\mathbf{u}_k = \mathbf{u}_{k-1} + \alpha_k \mathbf{p}_k$.
6. If $\mathbf{r}_k \approx \mathbf{0}$, stop; else go to step 2.

The preconditioner matrix $\mathbf{P}$ is selected as the incomplete Cholesky factorization of the matrix $\mathbf{K}$. That is $\mathbf{P} = \mathbf{L}\mathbf{L}^T \approx \mathbf{K}$. In this work, the matrix $\mathbf{L}$ is designed as follows:

$$\mathbf{L} = \begin{bmatrix} \mathbf{L}_{11} & \mathbf{0} & \mathbf{0} & \mathbf{0} \\ \mathbf{L}_{21} & \mathbf{L}_{22} & \mathbf{0} & \mathbf{0} \\ \mathbf{L}_{31} & \mathbf{L}_{32} & \mathbf{L}_{33} & \mathbf{0} \\ \mathbf{L}_{41} & \mathbf{L}_{42} & \mathbf{L}_{43} & \mathbf{L}_{44} \end{bmatrix} \in \Re^{4wh \times 4wh}. \tag{6}$$

where the submatrices $\mathbf{L}_{ij}$ are all of size $wh \times wh$. The detailed structure and formulas in getting the entries of $\mathbf{L}_{ij}$ can be obtained in [3] with some modifications.

In our numerical minimization algorithm, the parameters w_i, $\alpha_{x,i}$, $\alpha_{y,i}$, $\beta_{x,i}$, $\beta_{y,i}$, $\gamma_{x,i}$, $\gamma_{y,i}$, $\delta_{x,i}$ and $\delta_{y,i}$ are initially set to 1 and then updated after a fixed number of the incomplete Cholesky preconditioned conjugate gradient (ICPCG) iterations. This manner yields good performance in our experiments.

4. EXPERIMENTAL RESULTS

The experimental results of using our optical flow estimation algorithm on a synthetic image sequence, *Yosemite* sequence, are presented here. This image sequence is very challenging owing to that it contains brightness variations in the sky region, motion discontinuities between sky and mountain region, and large image motions at the lower-left corner of the sequence. Fig. 1(a) displays one frame from this sequence and Fig. 1(b) depicts the estimated motion field by using our algorithm. From Fig. 1(b), one can see that our algorithm can produce distinct motion boundaries between the sky and mountain region and yields accurate motion field in the sky region. Estimated brightness variations of the *Yosemite* sequence is shown in Fig. 1(c). This figure indicates that this sequence gets brighter at the left part of the sky region and becomes darker at the right part of this region as we observe in this image sequence. To compare with other techniques, we adopted the angular error measure used by Barron et al. [2] as our performance measure. Table 1 lists the results of our algorithm as well as other techniques reported in literature. Because some researchers only reported their results on the sky-excluded *Yosemite* sequence, thus we also list our results for the sky-excluded *Yosemite* sequence in Table 1. To our knowledge, Farnebäck's method [7] has the best performance for the sky-excluded *Yosemite* sequence reported to date in literature. Our method has a larger average angular error but smaller standard deviation than Farnebäck's method. Considering the average angular error and the standard deviation simultaneously, our algorithm is still comparable to Farnebäck's method for the sky-excluded *Yosemite* sequence. For the sky-included *Yosemite* sequence, our algorithm has the best performance among the techniques shown in Table 1.

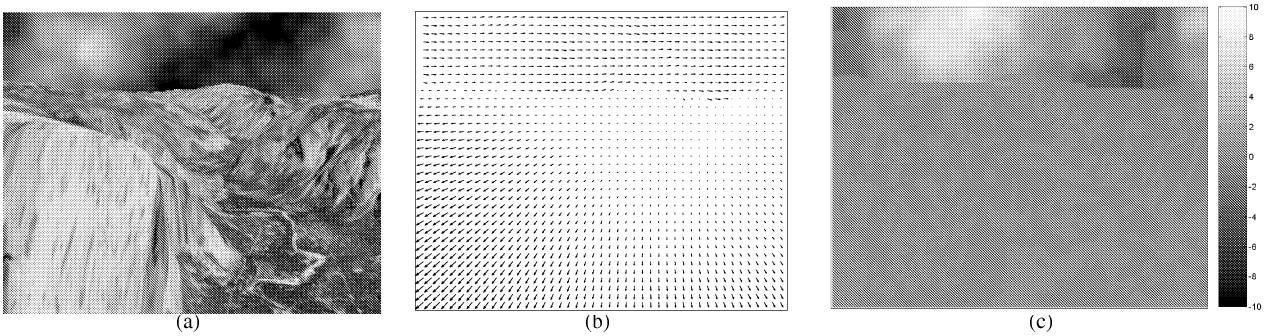

(a) (b) (c)

Fig. 1. Experimental results of *Yosemite* sequence. (a) One frame from this sequence. (b) Computed motion field. (c) Estimated brightness variations. (Brightness variation is defined as $-mI - c$.)

5. CONCLUSION

In this paper, we developed a very accurate gradient-based regularization algorithm for optical flow computation with non-uniform brightness variations. Our algorithm was constructed from the GDIM-based optical flow constraint and two auxiliary estimation schemes: the robust estimation and dynamic smoothness adjustment. We adopted GDIM to cope with the problem of brightness variations and applied robust estimation to reduce the influence of unreliable image flow constraints. We proposed a dynamic smoothness adjustment scheme to effectively suppress the smoothness constraint in the vicinity of motion discontinuities, thereby yielding more distinct motion boundaries. The solution of the resulting linear system for the above optical flow regularization problem was obtained by using an efficient numerical algorithm, i.e., the incomplete Cholesky preconditioned conjugate gradient algorithm. Experimental results on some synthetic and real image sequences showed that our method produces nearly the most accurate optical flow estimation among the techniques reported to date in literature.

Table 1. Summary of *Yosemite* Results

Technique	Avg. error (deg)	St. dev. (deg)	Density (%)
Horn and Schunck (modified)	9.78	16.19	100
Uras et al. (unthresholded)	8.94	15.61	100
Nagel	10.22	16.51	100
Anandan (unthresholded)	13.36	15.64	100
Zhang et al.	5.59	11.24	100
Alvarez et al.	5.53	7.40	100
Ong and Spann	5.79	12.55	89.9
Odobez and Bouthemy	6.17	12.61	98.1
Srinivasan and Chellappa	8.94	10.63	100
Liu et al.	6.84	12.88	100
Lai and Vemuri (gradient-based)	7.81	14.57	100
Proposed method	**2.70**	**5.20**	**100**
Mémin and Pérez*	1.58	1.21	100
Lai and Vemuri (SSD-based)*	2.04	1.52	100
Farnebäck*	1.14	2.14	100
Proposed method*	**1.52**	**1.27**	**100**

* The sky region is excluded in the computation of error for these techniques.

6. REFERENCES

[1] B. K. P. Horn and B. G. Schunck, "Determining optical flow," *Artificial Intelligence*, vol. 17, pp. 185–203, 1981.

[2] J. L. Barron, D. J. Fleet, and S. S. Beauchemin, "System and experiment performance of optical flow techniques," *International Journal of Computer Vision*, vol. 12, no. 1, pp. 43–77, 1994.

[3] S. H. Lai and B. C. Vemuri, "Reliable and efficient computation of optical flow," *International Journal of Computer Vision*, vol. 29, no. 2, pp. 87–105, 1998.

[4] S. Negahdaripour, "Revised definition of optical flow: Integration of radiometric and geometric cues for dynamic scene analysis," *IEEE Trans. Pattern Anal. Machine Intell.*, vol. 20, no. 9, pp. 961–979, Sept. 1998.

[5] M. J. Black and P. Anandan, "The robust estimation of multiple motions: Parametric and piecewise-smooth flow fields," *Computer Vision and Image Understanding*, vol. 63, no. 1, pp. 75–104, 1996.

[6] G. Li, "Robust regression," in *Exploring Data Tables, Trends, and Shapes*, D. C. Hoaglin, F. Mosteller, and J. W. Tukey, Eds., pp. 281–343. Wiley, New York, 1985.

[7] Farnebäck, "Very high accuracy velocity estimation using orientation tensors, parametric motion, and simultaneous segmentation of the motion field," in *Proceedings of International Conference on Computer Vision*, 2001, pp. 171–177.